Langmuir

Article

pubs.acs.org/Langmuir

Construction of a Semiconductor–Biological Interface for Solar Energy Conversion: p-Doped Silicon/Photosystem I/Zinc Oxide

Jeremiah C. Beam,[†] Gabriel LeBlanc,[†] Evan A. Gizzie,[†] Borislav L. Ivanov,[‡] David R. Needell,[†] Melinda J. Shearer,[†] G. Kane Jennings,[§] Charles M. Lukehart,*[,†] and David E. Cliffel*[,†]

[†]Department of Chemistry, [‡]Department of Physics and Astronomy, and [§]Department of Chemical and Biomolecular Engineering, Vanderbilt University, Nashville, Tennessee 37235, United States

Supporting Information

ABSTRACT: The interface between photoactive biological materials with two distinct semiconducting electrodes is challenging both to develop and analyze. Building off of our previous work using films of photosystem I (PSI) on p-doped silicon, we have deposited a crystalline zinc oxide (ZnO) anode using confined-plume chemical deposition (CPCD). We demonstrate the ability of CPCD to deposit crystalline ZnO without damage to the PSI biomaterial. Using electrochemical techniques, we were able to probe this complex semiconductor–biological interface. Finally, as a proof of concept, a solid-state photovoltaic device consisting of p-doped silicon, PSI, ZnO, and ITO was constructed and evaluated.

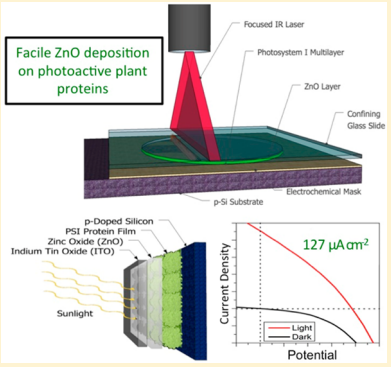

INTRODUCTION

Over the course of billions of years of evolution, nature has developed a remarkable set of nanomaterials capable of photochemical conversion with efficiencies not currently possible using man-made materials. Of particular interest for solar energy conversion is a membrane protein found in the thylakoids of higher-order plants known as photosystem I (PSI). PSI is capable of photoexciting electrons with an internal quantum efficiency near unity.[1] This efficiency, coupled with its natural abundance and ease of extraction, has led researchers across the globe to integrate this biomaterial into photovoltaic and photoelectrochemical devices.[2−4]

The efficiency of PSI stems from its ability to quickly transport the photoexcited electron from the P700 reaction center (located on the luminal side of the membrane) to the F_B site (located on the stromal side of the membrane) through an internal electron transfer chain. This separates the photo-induced electron–hole pair both spatially and energetically. In nature the photoexcited electron is collected by the water-soluble redox protein ferredoxin, while the water-soluble redox protein plastocyanin delivers another electron to the oxidized P700 reaction center.[5] In artificial biohybrid devices, these redox proteins are replaced with electrodes and electrochemical mediators.[2]

While metal electrodes have traditionally been used in artificial PSI devices, semiconducting electrodes have been shown to provide significant improvements in photocurrent and photovoltage production.[6−13] p-doped silicon was found to be an excellent platform for electron donation to the P700 reaction center.[11] Additionally, Mershin and co-workers found that ZnO was able to accept the electrons from the F_B site of PSI.[12] Furthermore, because of the large band gap in ZnO, this semiconductor is transparent to visible light and can therefore serve as the transparent electrode, allowing light to reach the photoactive layer. We now report the fabrication of an electrochemically active p-doped silicon/PSI/ZnO multilayer electrode and the incorporation of this electrode into a functional p-doped silicon/PSI/ZnO/ITO solid-state photovoltaic device (Figure 1).

Simultaneously interfacing a PSI film with p-doped silicon and n-type ZnO presents several challenges. Due to the organic nature of PSI, any high-temperature processing and harsh

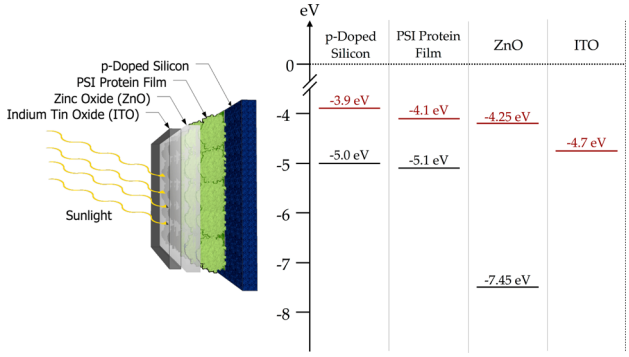

Figure 1. Illustration of the various components in the reported solid-state device along with their band energies.

Received: June 25, 2015
Revised: August 25, 2015
Published: August 28, 2015

DOI: 10.1021/acs.langmuir.5b02334
Langmuir 2015, 31, 10002−10007

chemical treatments must be performed prior to PSI film deposition. In other words, one of the semiconductors will need to be deposited under mild conditions. We address this issue by employing a relatively new deposition technique known as confined-plume chemical deposition (CPCD) to fabricate PSI/ZnO bilayers which exhibit good electrical contact.[14] These bilayers were then incorporated into a functional p-doped silicon/PSI/ZnO/ITO solid-state photovoltaic device.

To our knowledge, this is the first demonstration of depositing a crystalline ZnO film directly onto a biological material without the use of seeding crystals. Additionally, it represents one of only a few reported methods for incorporating PSI reaction centers into a solid-state device and the only one using two semiconducting electrodes to maximize the unidirectional current flow through the PSI layer.[15,16]

EXPERIMENTAL SECTION

Preparation of Substrates. Lightly p-doped (boron dopant density = 10^{16} cm^{-3}) silicon substrates were purchased from University Wafer (Boston, MA). In most experiments, the silicon substrate was used as received. For specific experiments (as described in the text) the native oxide layer on the silicon substrate was etched with a 2% hydrogen fluoride solution. (***Caution!*** Hydrogen fluoride is extremely corrosive and dangerous.) Proper protective equipment and procedures should always be used. Immediately following etching, the silicon substrates were rinsed with copious amounts of deionized water.

Extraction of Photosystem I. Photosystem I complexes from commercially available baby spinach were isolated using previously described methods. Briefly, thylakoid membranes were isolated from spinach leaves via maceration and subsequent centrifugation at 4000*g*.[17] The PSI complex was then removed from the thylakoid membrane by adding a high concentration of surfactant, followed by further centrifugation.[18] The protein was then purified using a chilled hydroxyapatite column. Following elution, excess surfactant and salt were removed via dialysis.[19] The concentration of the resulting PSI solution consisted of 1.7×10^{-6} M active P700 reaction centers with a chlorophyll a/b ratio of 3.5 as characterized by the methods of Porra and Baba et al., respectively.[20,21]

Modification of Substrates with Photosystem I. Films of PSI were deposited onto the silicon substrates following the procedure previously developed by Ciesielski and co-workers.[22] Briefly, 60 or 160 μL of PSI extract solution was pipetted onto the silicon substrate (exposed area of 0.385 or 1.000 cm^2), and a vacuum was applied to remove any solvent. Due to the low surfactant concentration in the protein suspension, the resulting protein film was no longer water soluble and could withstand electrochemical experiments using aqueous mediators. The thickness of the protein film can be easily increased by adding additional deposition steps or decreased by diluting the concentration of the initial solution. Film thicknesses were determined using a Vecco Dektak 150 stylus profilometer. For these measurements the protein film was scratched to the underlying silicon substrate, and the profilometer step height from the top of the film to the underlying substrate was used to determine the average thickness of the films (~0.5 μm).

CPCD of ZnO. CPCD was performed following the same concept described by Ivanov and co-workers.[14] Here, the ZnO precursor, $Zn_5(CO_3)_2(OH)_6$ (hydrozincite), was synthesized by a method similar to that of Wahab and co-workers.[23] Hydrozincite was suspended in benzene (10 mM) and drop cast onto the PSI-modified silicon electrode (10 μL). After drying in air, the sample was confined using a glass slide and a custom-made aluminum frame. The sample was then irradiated using a tabletop 2.94 μm Er:YAG (yttrium aluminum garnet) laser with a pulse duration of 150 μs. The laser was focused using a cylindrical ZnSe lens resulting in a beam area roughly 500 μm × 12.5 mm. The laser, with an energy output of 100 mJ, was pulsed at 20 Hz and was scanned twice over the surface of the sample at a rate of 317 μm s^{-1}. The sample was then removed from confinement, and compressed air was used to remove excess ZnO and carbon material.

ZnO Characterization. After modification with ZnO, the samples were characterized using a number of analytical techniques. SEM was performed using a Hitachi S4200 at an accelerating voltage of 10 kV. Energy-dispersive X-ray analysis was performed using a Zeiss Merlin at an accelerating voltage of 10 kV. Powder X-ray diffraction scans were obtained on a Scintag X1 θ/θ automated powder X-ray diffractometer with a Cu target (1.5418 Å), a Peltier-cooled solid-state detector, and a zero-background Si(510) sample support.

Electrochemical Measurements. Electrochemical measurements were performed using a CH Instruments (Austin, TX) CHI 660a electrochemical workstation. The silicon substrate was set as the working electrode, Ag/AgCl (3 M KCl) was used as the reference electrode, and platinum mesh was used as a counter electrode. Electrochemical mediator solutions consisted of 100 mM potassium chloride (Sigma-Aldrich) and 2 mM hexaammineruthenium(III) chloride (RuHex) (Sigma-Aldrich) or 2 mM methyl viologen dichloride hydrate (MV) (Sigma-Aldrich).

Solid-State Device Fabrication. Solid-state devices were fabricated using ITO-coated PET (60 Ω $square^{-1}$, Sigma-Aldrich) to make electrical contact with the ZnO layer. In order to generate as much contact as possible with the rough ZnO layer, a small piece of transparent PET was pressed onto the flexible ITO electrode by sandwiching the layers between two pieces of glass and binding the system together with clips. Additional fabrication details, including photographs of devices, are provided in Figure S1. Photochronoamperometric experiments were performed at an overpotential of 0.00 V (vs Ag/AgCl). Illumination was provided using a 250 W cold light source (Leica KL 2500 LCD) equipped with a 633 nm high-pass filter generating a light intensity of 0.19 W cm^{-2}. In the case of solid-state devices, the reference and counter electrodes were both connected to the ITO electrode.

Current−Voltage (*i*−V) Measurements at Solar Simulation. *i*−V curves for solid-state devices were obtained using a Sciencetech SF150B solar simulator with an AM1.5G filter (class A spectral match, class B nonuniformity) connected to a Keithley 2400 source meter controlled by a custom-designed Labview software program. The samples were swept from −0.5 to 0.5 V at a step rate of 0.02 V. The lamp was calibrated to 1.00 full sun with a NREL certified silicon reference diode.

Internal Quantum Efficiency. UV−vis spectra were collected on a Varian Cary 5000 UV−vis−NIR spectrophotometer. A background of silicon and borosilicate glass was used to include only absorbance from PSI and ZnO. Incident photon conversion efficiency (IPCE) measurements were performed with a 6 W Fianium fiber laser supercontinuum source.

RESULTS AND DISCUSSION

Previous work has demonstrated that depositing PSI films onto p-doped silicon resulted in significant photocurrent enhancement when compared to more traditional metal electrodes (i.e., gold).[11] Unfortunately, this system required the electrochemical mediator methyl viologen (MV). In addition to the toxic nature of MV, the use of an electrochemical mediator produces a number of problems such as the corrosion of metal electrodes, limitations in the mass transfer of soluble mediators, and device failure caused by leaks. Therefore, the development of a solid-state device is much more appealing for practical applications.

To develop a solid-state system, a material with the proper energy alignment with the F_B site of PSI is critical to facilitating electron transfer. As seen in Figure 1, the conduction band of ZnO lies below the formal potential of PSI's F_B site. Unfortunately there are few, if any, reported methods for depositing a layer of ZnO that would be in sufficient contact with the rough film of PSI for efficient interfacial electron

DOI: 10.1021/acs.langmuir.5b02334
Langmuir 2015, 31, 10002−10007

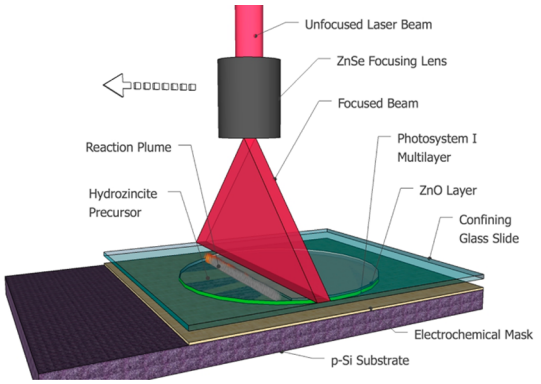

Figure 2. Illustration of the CPCD process used to generate a ZnO film on top of a biological PSI protein layer.

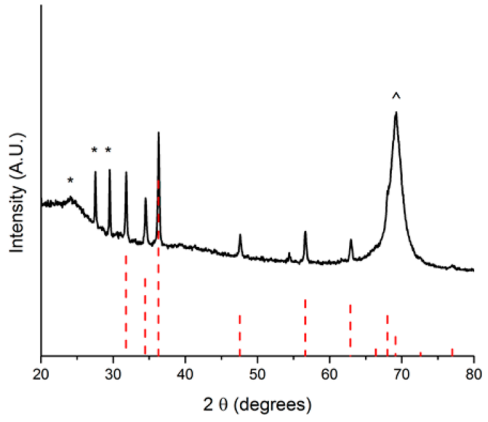

Figure 3. XRD pattern of ZnO/PSI/Si. Red dashed lines represent the bulk pattern of wurtzite ZnO (PDF no. 36-1451). Starred peaks (*) are diffraction from the electrochemical mask, and the peak labeled with a carat (^) is diffraction from the Si substrate.

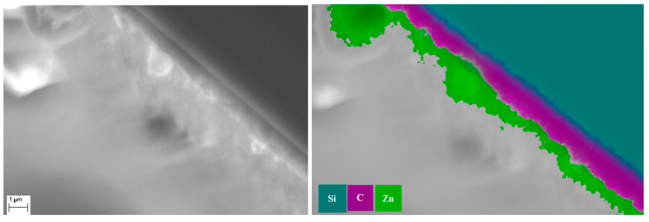

Figure 4. SEM micrograph (left) and EDS map (right) of layered Si/PSI/ZnO.

transport. While there are several methods for chemically depositing zinc oxide, all require temperatures greater than 70 °C.[23−25] Since the deposition of ZnO at these temperatures could denature the protein complex, an alternative deposition method must be investigated. Therefore, we employed a relatively new technique, CPCD, that has been used previously to rapidly deposit crystalline ReB_2, RuB_2, WB_4, and B_4C on various substrates without collateral thermal damage.[14]

In CPCD (Figure 2), the irradiation of appropriate molecular precursors spatially confined between two support plates by a beam of pulsed infrared (IR) laser light leads to rapid precursor decomposition, the formation of a visible reaction plume under spatial and temporal confinement, and the deposition of crystalline ceramic material of high purity as the laser beam is rastered across the specimen. Pulse energy analysis reveals that 75−95% of the IR light energy is absorbed during precursor

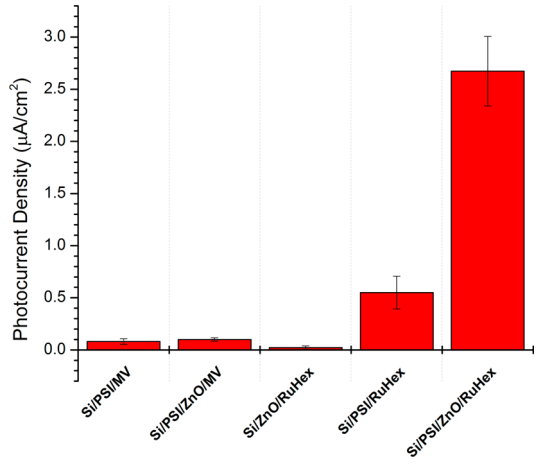

Figure 5. Average photocurrent density for various samples tested with RuHex or methyl viologen. The photocurrent density was determined by taking the current value after 10 s of illumination. The working electrode was held at the open circuit voltage of the system (Table S3).

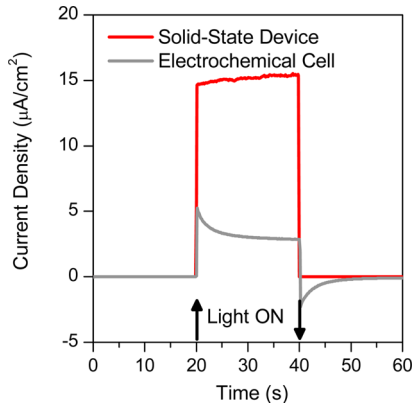

Figure 6. Photochronoamperometric analysis of a solid state device (red) compared to a wet electrochemical cell (gray). Both systems employed a working electrode consisting of Si/PSI/ZnO. In the wet electrochemical device, the electrolyte consisted of 2 mM RuHex and 100 mM KCl, and the counter electrode was Pt mesh. ITO-coated PET was used to make an electrical connection to the ZnO layer in the solid-state device, and both the reference and counter electrode connections were connected to the ITO.

decomposition, thus permitting the use of either hard or soft support materials. Rapid cooling of reaction plume species leads to the surface-nucleated growth of crystalline, ceramic microcrystals, without the need for subsequent thermal annealing.

CPCD of a hydrozincite $[Zn_5(CO_3)_2(OH)_6]$ solution drop cast onto a thin film of PSI on p-doped silicon forms a dull translucent film on the surface of the PSI layer. XRD analysis of this film reveals crystalline, wurtzite ZnO as the primary product (Figure 3). SEM images indicated that the ZnO forms a continuous particulate layer directly on the protein, as confirmed by energy-dispersive X-ray (EDS) analysis (Figure 4, Figure S2).

To confirm that CPCD processing leaves the underlying PSI film undamaged, photochronoamperometry was performed using an actinic light source. As seen in Figure 5, the deposition of a ZnO layer not only allows the PSI to remain photoactive but also significantly enhances the photocurrent density of the system when a hexaammineruthenium(iii) chloride (RuHex)

DOI: 10.1021/acs.langmuir.5b02334
Langmuir 2015, 31, 10002−10007

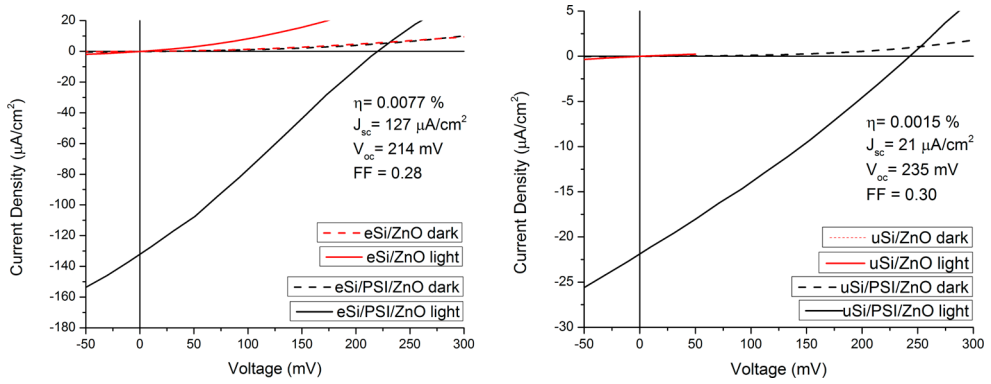

Figure 7. *i*–V analysis of a solid-state device composed of etched (left) and unetched (right) p-doped silicon, a film of PSI, CPCD ZnO, and an ITO contact and control samples composed of p-doped silicon, CPCD ZnO, and an ITO contact. Samples were tested under 1 sun illumination (red) and in the dark (black).

Table 1. Photocurrent Output (μA cm^{-2}) of Five Unetched Solid-State Devices over a Period of 2 Weeks

	Days After Fabrication									
Device	1	4	5	6	7	8	13	14	avg	RSD %
A	5.76	3.97	4.26	3.27	2.67	6.08	5.32	5.77	4.6 ± 1.3	28
B	3.41	4.19	4.41	3.69	4.07	4.5	4.8	3.96	4.1 ± 0.4	10
C	8.47	8.01	11.8	7.32	7.27	6.17	6.61	6.07	7.7 ± 1.9	25
D	16.1	21.1	17.3	16.4	14.2	14.4	10.6	11.9	15 ± 3	22
E	5.21	5.56	5.54	5.73	4.52	5.29	4.95	5.03	5.2 ± 0.4	7.7

mediator is employed. ZnO facilitates electron transfer from the F_B site of PSI to the RuHex mediator because the conduction band of ZnO (−4.25 eV) lies between the formal potentials of F_B and RuHex (−4.10 and −4.60 eV, respectively). When MV is used as a mediator, no enhancement is observed because the formal potential of MV (−4.05 eV) is higher than the conduction band of the ZnO. It is worth noting, however, that the photocurrent difference was insignificant between the samples with and without ZnO when MV was used, providing further evidence that CPCD deposition does not damage the PSI film. Higher photocurrents without a zinc oxide layer using methyl viologen as a mediator can be achieved by etching the silicon prior to the photochronoamperometry experiments.[11]

After observing this enhancement in photocurrent from the addition of a ZnO layer, the p-doped silicon/PSI/ZnO trilayer biohybrid electrode can be transformed into a solid-state photovoltaic device by placing ITO-coated PET in contact with the ZnO layer as an anodic electrode (Figure S1). Photochronoamperometric analysis (Figure 6) reveals that this device not only improves upon the photocurrent density but also changes the shape of the curve when compared to an electrochemical cell. The use of an electrochemical mediator introduces diffusional mass-transfer limitations in the cell as indicated by the time decay in the photocurrent, which follows Cottrell behavior for diffusion-controlled current, while the solid-state device does not have this decay in current.

With a solid-state device in hand, current–voltage (*I*–V) analysis revealed the efficiency and other performance metrics of this device under calibrated solar illumination (Figure 7). The unetched Si device had a photocurrent density of 21 μA cm^{-2} and an external efficiency of 0.0015%. When the p-doped silicon substrate was etched with hydrofluoric acid before the deposition of the PSI layer, a 6-fold improvement in the photocurrent density (127 μA cm^{-2}) and a 5-fold increase in the efficiency (0.0077%) of the final device were observed. Although the photocurrent density increased with the removal of the insulating SiO_2 layer, by lowering the internal resistance of the device, a drop in the open circuit voltage was also observed. This might be attributed to the loss of the Shottky barrier in the device. IPCE spectra were taken of devices with and without the presence of photosystem I, indicating that photosystem I is indeed the light-active portion of the device (Figure S4). Although the efficiencies for the above cells are low, this fabrication technique has an overall low cost and allows for the rapid preparation of devices. Further optimization of device architecture will likely provide further improvements in both efficiency and photocurrent density.

Of great concern when using a biological material in solar energy technology is device longevity. Previous photoelectrochemical devices employing PSI have shown consistent photocurrent values for over 280 days.[22] To address long-term performance, five solid-state devices were tested, after 10 s of illumination, over a period of 2 weeks (Table 1). Two of the devices (B and E) showed very good stability over the course of 2 weeks, with a reduction in less than 10% of the initial photocurrent. The other three (A, C, and D) showed less than a 30% reduction in initial photocurrent over a period of 2 weeks. Device exposure to long, intense light for over 67 h also resulted in no significant photocurrent degradation (Figure S5).

3. CONCLUSIONS

A method for the direct deposition of polycrystalline ZnO onto a photoactive biological material using a single-source precursor is described for the first time. This processing strategy is used to develop a solid-state solar cell with a unique semiconductor/biological interface. While the resulting interface is complex on the microscale, device preparation and testing are rapid and straightforward.

The resulting solid-state solar cell exhibits significant improvements in photocurrent production over a traditional photoelectrochemical cell and is stable for at least 2 weeks.

DOI: 10.1021/acs.langmuir.5b02334
Langmuir 2015, 31, 10002–10007

While the overall efficiency of the devices tested is relatively low, this study demonstrates an important proof of concept that will inevitably provide a pathway to more efficient devices based on the trajectory of other biohybrid electrodes.

More broadly, using CPCD to deposit crystalline materials on biological and other temperature-sensitive substrates without the need for seeding is beneficial for a variety of applications. Additionally, the use of electrochemical mediators to probe electronic interactions between semiconductor−biological interfaces has applications in several different fields, specifically biosensors and bioelectronics.

■ ASSOCIATED CONTENT

Supporting Information

The Supporting Information is available free of charge on the ACS Publications website at DOI: 10.1021/acs.langmuir.5b02334.

Additional data describing the fabrication and electrochemical characterization of solid-state devices and SEM images of the ZnO layer (PDF)

■ AUTHOR INFORMATION

Corresponding Authors

*Fax: +1 615 343 1234. Tel: +1 615 322 2935. E-mail: charles.m.lukehart@vanderbilt.edu.

*Fax: +1 615 343 1234. Tel: +1 615 343 3937. E-mail: d.cliffel@vanderbilt.edu.

Present Addresses

(G.L) The University of Tulsa, 430 South Gary Place, Keplinger Hall, Room L134A. Tulsa, OK 74104−9700

(M.J.S) University of Wisconsin-Madison, 1101 University Ave., Madison,WI 53706, United States.

(D.R.N) Calfornia Institute of Technology, 1200 E. California Blvd, Pasadena, CA 91125, United States.

Author Contributions

Authors J.C.B. and G.L. contributed equally to this work. The manuscript was written through the contributions of all authors. All authors have given approval to the final version of the manuscript.

Notes

The authors declare no competing financial interest.

■ ACKNOWLEDGMENTS

We gratefully acknowledge the financial support of the National Science Foundation (DMR0907619, DMR 1263182 (D.R.N)), the NSF EPSCoR (EPS 1004083), the United States Department of Agriculture (2013-67021-21029 USDA), the U.S. Environmental Protection Agency (SU8360221), Vanderbilt University for partial support through an IDEAS grant award, and the Scialog Program from the Research Corporation for Science Advancement. We also gratefully acknowledge J. Scott Niezgoda, Andrew G. Harris, and Maxwell Robinson for their assistance in data collection.

■ ABBREVIATIONS

PSI, photosystem I; ITO, indium tin oxide; CPCD, confined-plume chemical deposition; MV, methyl viologen dichloride hydrate; RuHex, hexaammineruthenium (iii) trichloride; Er:YAG, erbium-doped yttrium aluminum garnet; CV, cyclic voltammetry

■ REFERENCES

(1) Hogewoning, S. W.; Wientjes, E.; Douwstra, P.; Trouwborst, G.; van, I. W.; Croce, R.; Harbinson, J. Photosynthetic Quantum Yield Dynamics: From Photosystems to Leaves. *Plant Cell* **2012**, *24*, 1921−1935.

(2) LeBlanc, G.; Gizzie, E. A.; Yang, S.; Cliffel, D. E.; Jennings, G. K. Photosystem I Protein Films at Electrode Surfaces for Solar Energy Conversion. *Langmuir* **2014**, *30*, 10990−11001.

(3) Nagy, L.; Magyar, M.; Szabó, T.; Hajdu, K.; Giotta, L.; Dorogi, M.; Milano, F. Photosynthetic Machineries in Nano-Systems. *Curr. Protein Pept. Sci.* **2014**, *15*, 363.

(4) Nguyen, K.; Bruce, B. D. Growing Green Electricity: Progress and Strategies for Use of Photosystem I for Sustainable Photovoltaic Energy Conversion. *Biochim. Biophys. Acta, Bioenerg.* **2014**, *1837*, 1553−1566.

(5) Golbeck, J. *Photosystem I: The Light-Driven Plastocyanin: Ferredoxin Oxidoreductase*; Springer: Urbana, IL, 2006; Vol. *24*, p 764.

(6) Den Hollander, M.-J.; Magis, J. G.; Fuchsenberger, P.; Aartsma, T. J.; Jones, M. R.; Frese, R. N. Enhanced Photocurrent Generation by Photosynthetic Bacterial Reaction Centers through Molecular Relays, Light-Harvesting Complexes, and Direct Protein−Gold Interactions. *Langmuir* **2011**, *27*, 10282−10294.

(7) Kievit, O.; Brudvig, G. W. Direct Electrochemistry of Photosystem I. *J. Electroanal. Chem.* **2001**, *497*, 139−149.

(8) Kondo, M.; Iida, K.; Dewa, T.; Tanaka, H.; Ogawa, T.; Nagashima, S.; Nagashima, K. V. P.; Shimada, K.; Hashimoto, H.; Gardiner, A. T.; Cogdell, R. J.; Nango, M. Photocurrent and Electronic Activities of Oriented-His-Tagged Photosynthetic Light-Harvesting/Reaction Center Core Complexes Assembled onto a Gold Electrode. *Biomacromolecules* **2012**, *13*, 432−438.

(9) Mukherjee, D.; May, M.; Vaughn, M.; Bruce, B. D.; Khomami, B. Controlling the Morphology of Photosystem I Assembly on Thiol-Activated Au Substrates. *Langmuir* **2010**, *26*, 16048−16054.

(10) Terasaki, N.; Yamamoto, N.; Hiraga, T.; Yamanoi, Y.; Yonezawa, T.; Nishihara, H.; Ohmori, T.; Sakai, M.; Fujii, M.; Tohri, A.; Iwai, I.; Inoue, Y.; Yoneyama, S.; Minakata, M.; Enami, I. Plugging a Molecular Wire into Photosystem I: Reconstitution of the Photoelectric Conversion System on a Gold Electrode. *Angew. Chem., Int. Ed.* **2009**, *48*, 1585−1587.

(11) LeBlanc, G.; Chen, G.; Gizzie, E. A.; Jennings, G. K.; Cliffel, D. E. Enhanced Photocurrents of Photosystem I Films on P-Doped Silicon. *Adv. Mater.* **2012**, *24*, 5959−5962.

(12) Mershin, A.; Matsumoto, K.; Kaiser, L.; Yu, D.; Vaughn, M.; Nazeeruddin, M. K.; Bruce, B. D.; Graetzel, M.; Zhang, S. Self-Assembled Photosystem-I Biophotovoltaics on Nanostructured TiO_2 and ZnO. *Sci. Rep.* **2012**, *2*, 234.

(13) Frolov, L.; Rosenwaks, Y.; Richter, S.; Carmeli, C.; Carmeli, I. Photoelectric Junctions Between GaAs and Photosynthetic Reaction Center Protein. *J. Phys. Chem. C* **2008**, *112*, 13426−13430.

(14) Ivanov, B. L.; Wellons, M. S.; Lukehart, C. M. Confined-Plume Chemical Deposition: Rapid Synthesis of Crystalline Coatings of Known Hard or Superhard Materials on Inorganic or Organic Supports by Resonant IR Decomposition of Molecular Precursors. *J. Am. Chem. Soc.* **2009**, *131*, 11744−11750.

(15) Das, R.; Kiley, P.; Segal, M.; Norville, J.; Yu, A. Integration of Photosynthetic Protein Molecular Complexes in Solid-State Electronic Devices. *Nano Lett.* **2004**, *4*, 1079−1083.

(16) Gordiichuk, P. I.; Wetzelaer, G. A. H.; Rimmerman, D.; Gruszka, A.; de Vries, J. W.; Saller, M.; Gautier, D. A.; Catarci, S.; Pesce, D.; Richter, S.; Blom, P. W. M.; Herrmann, A. Solid-State Biophotovoltaic Cells Containing Photosystem I. *Adv. Mater.* **2014**, *26*, 4863−4869.

(17) Reeves, S. G.; Hall, D. O. [8] Higher Plant Chloroplasts and Grana: General Preparative Procedures (Excluding High Carbon Dioxide Fixation Ability Chloroplasts). *Methods in Enzymology*; Academic Press: New York, 1980; Vol. *69*, pp 85−94.

(18) Ciobanu, M.; Kincaid, H. A.; Jennings, G. K.; Cliffel, D. E. Photosystem I Patterning Imaged by Scanning Electrochemical Microscopy. *Langmuir* **2005**, *21*, 692−698.

DOI: 10.1021/acs.langmuir.5b02334
Langmuir 2015, 31, 10002−10007

(19) Ciesielski, P. N.; Faulkner, C. J.; Irwin, M. T.; Gregory, J. M.; Tolk, N. H.; Cliffel, D. E.; Jennings, G. K. Enhanced Photocurrent Production by Photosystem I Multilayer Assemblies. *Adv. Funct. Mater.* **2010**, *20*, 4048−4054.
(20) Porra, R. J. The Chequered History of the Development and Use of Simultaneous Equations for the Accurate Determination of Chlorophylls a and B. *Photosynth. Res.* **2002**, *73*, 149−156.
(21) Baba, K.; Itoh, S.; Hastings, G.; Hoshina, S. Photoinhibition of Photosystem I Electron Transfer Activity in Isolated Photosystem I Preparations with Different Chlorophyll Contents. *Photosynth. Res.* **1996**, *47*, 121−130.
(22) Ciesielski, P. N.; Hijazi, F. M.; Scott, A. M.; Faulkner, C. J.; Beard, L.; Emmett, K.; Rosenthal, S. J.; Cliffel, D.; Jennings, G. K. Photosystem I - Based Biohybrid Photoelectrochemical Cells. *Bioresour. Technol.* **2010**, *101*, 3047−3053.
(23) Wahab, R.; Ansari, S. G.; Kim, Y. S.; Dar, M. A.; Shin, H. S. Synthesis and Characterization of Hydrozincite and its Conversion Into Zinc Oxide Nanoparticles. *J. Alloys Compd.* **2008**, *461*, 66−71.
(24) Weintraub, B.; Deng, Y.; Wang, Z. L. Position Controlled Seedless Growth of ZnO Nanorod Arrays on a Polymer Substrate vis Wet Chemical Synthesis. *J. Phys. Chem. C* **2007**, *111*, 10162−10165.
(25) Huang, M. H.; Wu, Y.; Feick, H.; Tran, N.; Weber, E.; Yang, P. Catalytic Growth of Zinc Oxide Nanowire by Vapor Transit. *Adv. Mater.* **2001**, *13*, 113−116.

DOI: 10.1021/acs.langmuir.5b02334
Langmuir 2015, 31, 10002−10007